J|A|C|S
ARTICLES
Published on Web 04/03/2002

Identification of the Metal Ion Binding Site on an RNA Motif from Hammerhead Ribozymes Using ^{15}N NMR Spectroscopy

Yoshiyuki Tanaka,[†,‡,§] Chojiro Kojima,[⊥,∞] Eugene H. Morita,[∥,#] Yasuhiro Kasai,[†] Kazuhiko Yamasaki,[†] Akira Ono,[⊥] Masatsune Kainosho,[⊥] and Kazunari Taira*[,†,¶]

Contribution from the Gene Discovery Research Center, National Institute of Advanced Industrial Science and Technology, Tsukuba Central 4, 1-1-1 Higashi, Tsukuba, Ibaraki 305-8562, Japan, Japan Science and Technology Corporation, Kawaguchi, Saitama 332-0012, Japan, Department of Chemistry, Graduate School of Science, Tokyo Metropolitan University, Hachioji, Tokyo 192-0397, and CREST, Japan, Graduate School of Biological Science, Nara Institute of Science and Technology, Ikoma, Nara 630-0101, Japan, Center for Gene Research, Ehime University, Matsuyama, Ehime 790-8566, Japan, Venture Business Laboratory, Ehime University, Matsuyama, Ehime 790-8577, Japan, and Department of Chemistry and Biotechnology, School of Engineering, The University of Tokyo, 7-3-1 Hongo, Tokyo 113-8656, Japan

Received June 22, 2001

Abstract: An RNA oligomer, r(GGACGAGUCC), which mimics the metal ion-binding motif of hammerhead ribozymes, was shown to fold by itself into a conformation possessing a metal ion binding property which is similar to that of the intact ribozyme (Tanaka, et al. *J. Am. Chem. Soc.* **2000**, *122*, 11303−11310). To determine the metal ion-binding site of this motif at an atomic level, we synthesized a series of RNA oligomers which were selectively labeled with a ^{15}N-labeled guanosine at each of the four guanosine residues. The ^{15}N-chemical shift perturbation with Cd(II) ions by one-dimensional (1D) ^{15}N NMR spectra showed that the chemical shift of the N7 of the G7 residue, N7/G7, in the metal ion-binding motif was specifically perturbed. This is the first experimental evidence to prove that the N7/G7 binds with a Cd(II) ion.

Metal ions are important cofactors for biologically active RNA molecules. A metal ion binding motif of hammerhead ribozymes is one of the most characterized motifs.[1] This motif comprises the G12-A9 pair and the flanking C11.1-G10.1 pair (so-called A9-G10.1 motif), and the N7 atom of the G10.1 residue is the metal ion binding site[1a−c,g] (Figure 1). It is also known that the motif can capture a wide range of divalent cations such as Mg(II), Cd(II), Co(II), Ca(II), and Mn(II), and hammerhead ribozymes are active when these divalent cations are bound to the motif during the catalytic reactions.[1d−g] It also should be noted that identical and similar sequence motifs are included in ribosomal RNA (rRNA)[2] and it is obviously important to study this motif.

NMR spectroscopy is perhaps the best technique for determining metal ion interaction sites on RNA molecules with atomic resolution. There have been several studies on metal ion-RNA interactions using ^{1}H and ^{13}C NMR spectroscopy.[1i,3] Although the metal ion-binding area could be estimated from these studies, ^{1}H and ^{13}C nuclei only indirectly probe the ion-binding, and consequently it is difficult to determine the metal ion-binding atom unambiguously. On the other hand, ^{15}N NMR spectroscopy provides direct experimental information on intermolecular interactions such as hydrogen bonding in nucleic acids[4] and metal ion-coordination in a protein and a porphyrin related compound.[5] Although several studies successfully applied ^{15}N NMR spectroscopy to detect the metal ion-binding to nucleosides and ATP,[6] we applied this NMR technique to detect

* Address correspondence to this author at The University of Tokyo. Phone: 81(Japan)-3-5841-8828 or 81(Japan)-298-61-3015. Fax: 81-3-5841-8828 or 81-298-61-3019. E-mail: taira@chembio.t.u-tokyo.ac.jp.
† National Institute of Advanced Industrial Science and Technology.
‡ Japan Science and Technology Corporation.
§ Present Address: Graduate School of Pharmaceutical Science, Tohoku University, Aobayama, Aoba-ku, Sendai 980-8578, Japan.
⊥ Tokyo Metropolitan University.
∞ Present address: Graduate School of Biological Science, Nara Institute of Science and Technology, Ikoma, Nara 630-0101, Japan.
∥ Center for Gene Research, Ehime University.
Venture Business Laboratory, Ehime University.
¶ The University of Tokyo.

(1) (a) Pley, H. W.; Flaherty, K. M.; McKay, D. B. *Nature* **1994**, *372*, 68−74. (b) Scott, W. G.; Murray, J. B.; Arnold, J. R. P.; Stoddard, B. L.; Klug, A. *Science* **1996**, *274*, 2065−2069. (c) Murray, J. B.; Terwey, D. P.; Maloney, L.; Karpeisky, A.; Usman, N.; Beigelman, L.; Scott, W. G. *Cell* **1998**, *92*, 665−673. (d) Scott, E. C.; Uhlenbeck, O. C. *Nucleic Acids Res.* **1999**, *27*, 479−484. (e) Wang, S.; Karbstein, K.; Peracchi, A.; Beigelman, L.; Herschlag, D. *Biochemistry* **1999**, *38*, 14363−14378. (f) Yoshinari, K.; Taira, K. *Nucleic Acids Res.* **2000**, *28*, 1730−1742. (g) Hunsicker, L. M.; DeRose, V. J. *J. Inorg. Biochem.* **2000**, *80*, 271−281. (h) Maderia, M.; Hunsicker, L. M.; DeRose, V. J. *Biochemistry* **2000**, *39*, 12113−12120. (i) Tanaka, Y.; Morita, E. H.; Hayashi, H.; Kasai, Y.; Tanaka T.; Taira, K. *J. Am. Chem. Soc.* **2000**, *122*, 11303−11310.
(2) Gautheret, D.; Konings, D.; Gutell, R. R. *J. Mol. Biol.* **1994**, *242*, 1−8.
(3) (a) Legault, P.; Hoogstraten, C. G.; Metlitzky, E.; Pardi, A. *J. Mol. Biol.* **1998**, *284*, 325−335. (b) Schmitz, M.; Tinoco, I., Jr. *RNA* **2000**, *6*, 1212−1225. (c) Butcher, S. E.; Allain, F. H.-T.; Feigon, J. *Biochemistry* **2000**, *39*, 2174−2182.
(4) (a) Gaffney, B. L.; Kung, P.-P.; Wang, C.; Jones R. A. *J. Am. Chem. Soc.* **1995**, *117*, 12281−12283. (b) Zhang, X.; Gaffney, B. L.; Jones R. A. *J. Am. Chem. Soc.* **1998**, *120*, 6625−6626. (c) Dingley, A. J.; Grzesiek, S. *J. Am. Chem. Soc.* **1998**, *120*, 8293−8297. (d) Pervushin, K.; Ono, A.; Fernández, C.; Szyperski, T.; Kainosho, M.; Wüthrich, K. *Proc. Natl. Acad. Sci. U.S.A.* **1998**, *95*, 14147−14151. (e) Tanaka, Y.; Kojima, C.; Yamazaki, T.; Kodama, T. S.; Yasuno, K.; Miyashita, S.; Ono, A. M.; Ono, A. S.; Kainosho M.; Kyogoku, Y. *Biochemistry* **2000,** *39*, 7074−7080.

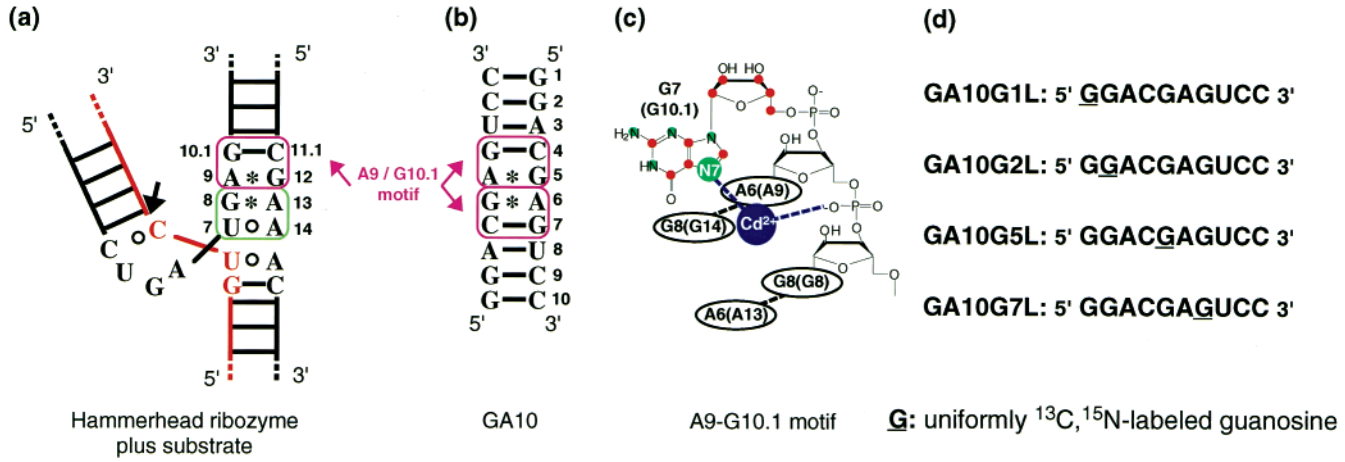

Figure 1. Sequences and secondary structures of (a) hammerhead ribozyme[1a−c] and (b) GA10 with numbering systems. The metal ion-binding motifs (A9-G10.1 motifs of hammerhead ribozymes and GA10) and the adjacent similar motif in hammerhead ribozymes are surrounded by magenta and green lines, respectively. In part a, the enzyme and substrate strands with conserved sequences are shown in black and red, respectively, and the cleavage site is indicated by a black arrow. In parts a and b, Watson−Crick base-pairs, non-Watson−Crick base-pairs, and shared-type G−A pairs are indicated by bars, open circles, and asterisks, respectively. (c) Schematic representation of the A9-G10.1 motif, as revealed by X-ray crystallography.[1a−c] The position of the Cd(II) ion is shown in blue, and is linked to binding sites via blue dashed lines. The tandem G−A pairs are indicated by black dashed lines with residue names in GA10 (those in hammerhead ribozymes are also indicated in parentheses). The isotopically labeled nuclei are highlighted (^{15}N, green; ^{13}C, red; ^{113}Cd, blue). (d) The names of labeled samples are indicated with the labeled residues underlined. They are named according to the positions of the uniformly ^{15}N- and ^{13}C-labeled guanosine residues (e.g., the G1 residue of GA10 is substituted by Labeled guanosine in GA10G1L).

the interaction between metal ions and a functional RNA oligomer for the first time.

Results

In our previous paper, we found that the A9-G10.1 motif can function as a metal ion-binding motif in the absence of other conserved residues of hammerhead ribozymes, and it was suggested that N7 of G7 (N7/G7), which corresponds to G10.1 in the hammerhead ribozyme, is a metal ion-binding site.[1i] To unambiguously determine the metal ion-binding site, the nitrogen nuclei of the guanosines in GA10 were ^{15}N-enriched (Figure 1). The carbon nuclei of the guanosines were also ^{13}C-enriched to allow identification of all nonexchangeable protons and to study the correlations between the N7 nuclei and the adjacent nuclei of base protons (H8) and carbons (C8) in the Cd(II) titration experiment. To simplify the spectral interpretation, we synthesized four different oligomers (i.e., GA10G1L, GA10G2L, GA10G5L, and GA10G7L; see Figure 1) in which a single guanosine was labeled with the naming reflecting the labeled residue number (Figure 1d).

Before measuring ^{15}N NMR spectra, we performed the equilibrium analysis of the GA10-$CdCl_2$ system with ^{1}H NMR spectra. This is because we had to know the binding behavior of Cd(II) ions to the motif for the interpretation of chemical shift changes of ^{15}N-nuclei. From this analysis, it was found that the binding of Cd(II) to two independent metal ion-binding motifs was asymmetric despite the 2-fold symmetry of the GA10(duplex) (Figure 2). For example, the resonance of H8/A6 was not perturbed until the molar ratio of [$CdCl_2$]/[GA10(duplex)] was approximately 1.0; however, above this point the resonance began to be perturbed and exhibited a transition curve (Figures 2 and 3). In contrast, other resonances were perturbed considerably before reaching the ratio of 1.0 (Figures 2 and 3). This probably indicates that the resonance of H8/A6 was insensitive to the first metal ion-binding, and sensitive to the second metal ion-binding. Hence, at least a three-state-equilibrium system was required to describe the binding process, and it is well-known that structural changes of short oligonucleotides are coorperative.[8] Accordingly, Cd(II) binding isotherms for ^{15}N-nuclei and other nuclei should also be biphasic. In view of the secondary structure, the two metal ion-binding motifs in GA10 are symmetric; however, the binding of the metal ion to the first binding site induces the structural perturbations around the second binding site.

Then we measured ^{15}N-chemical shift changes versus Cd(II) ion concentrations (Figure 4). Experimental ^{15}N-chemical shifts for N7-nuclei and theoretical curves based on the above equilibrium system are presented in Figure 5. The N7/G7 resonance was shifted toward high-field by 19.6 ppm upon addition of Cd(II) ion (the molar ratio of [$CdCl_2$]/[GA10(duplex)] = 6.0), whereas those of the other nitrogen atoms (N1, N2, N3, and N9 of G7) were not shifted significantly (Figures 4 and 5). Furthermore, only small shifts were observed for the N7 resonances of the guanosine residues outside of the metal ion-binding motif. For example, N7/G1 and N7/G2 showed 4.8 and 5.9 ppm high-field shifts ([$CdCl_2$]/[GA10(duplex)] = 5.0), respectively (Figures 4 and 5).

It was also demonstrated that all the ^{15}N-chemical shift changes were accountable for the equilibrium system revealed

(5) (a) Damblon, C.; Prosperi, C.; Lian, L.-Y.; Barsukov, I.; Soto, R. P.; Galleni, M.; Frere, J.-M.; Roberts G. C. K. *J. Am. Chem. Soc.* **1999**, *121*, 11575−11576. (b) Jakobsen, H. J.; Ellis, P. D.; Inners, R. R.; Jensen, C. F. *J. Am. Chem. Soc.* **1982**, *104*, 7442−7452.
(6) (a) Buchanan, G. W.; Stothers, J. B. *Can. J. Chem.* **1982**, *60*, 787−791. (b) Buchanan, G. W.; Bell, M. J. *Can. J. Chem.* **1983**, *61*, 2445−2448. (c) Happe, J. A.; Morales, M. *J. Am. Chem. Soc.* **1966**, *88*, 2077−2078.
(7) (a) SantaLucia, J., Jr.; Kierzek, R.; Turner, D. H. *J. Am. Chem. Soc.* **1991**, *113*, 4313−4322. (b) Ono, A.; Tate, S.; Kainosho, M. New strategy for stable-isotope-aided multidimensional NMR spectroscopy of DNA oligomers. In *Stable Isotope Applications in Biomolecular Structure and Mechanisms*; Trewhella, et al., Eds.; Los Alamos National Laboratory: Los Alamos, NM, 1994; pp 127−144.
(8) (a) Sugeta, H. *Bull. Chem. Soc. Jpn.* **1981**, *54*, 3706−3710. (b) Kodama, T. S.; Yasuno, K.; Tanaka, Y.; Kawamura, A.; Kojima, C.; Sugeta H.; Kyogoku Y. *Prog. Biophys. Mol. Biol.* **1996**, *65*, 136 (Suppl. 1) (c) Kodama, T. S.; Kyogoku, Y.; Sugeta, H. A novel method for estimating thermodynamic parameters in multi-equilibrium systems by global analysis of spectrophotometric data. In *Spectroscopy of Biological Molecules; Modern Trends*; Carmona, P., Navarro, R., Hernanz, A., Eds.; Kluwer Academic Publishers: Dordrecht, The Netherlands, 1997; pp 577−578.

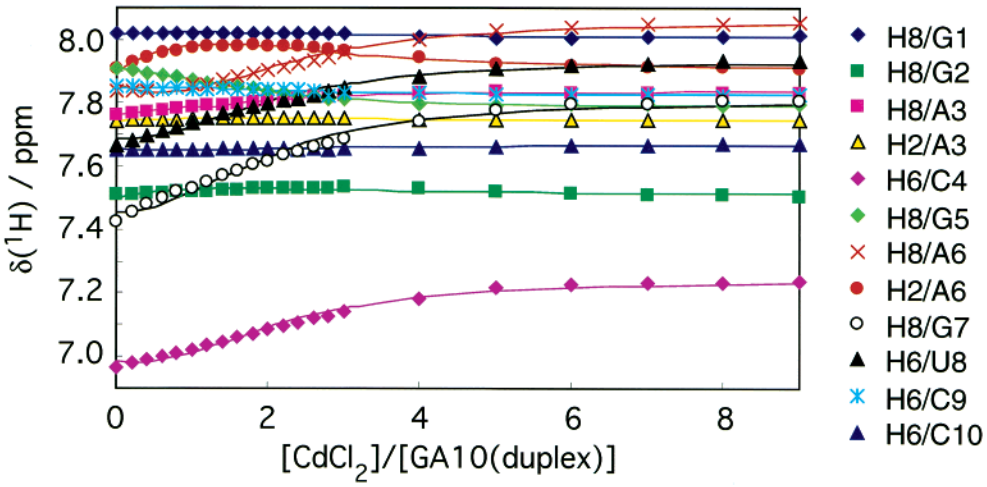

Figure 2. The chemical shift values of base protons (H8, H2, and H6) are plotted against molar ratio ([Cd(II)]/[GA10(duplex)]). Theoretical curves were generated by the fitting as described previously[8] and presented in the figure. From the nonlinear least-squares regression, apparent dissociation constants for the first and the second metal ion-binding constants (Kd_{1app} and Kd_{2app}) were calculated to be $3.2 \times 10^{-4} \pm 0.2 \times 10^{-4}$ and $3.3 \times 10^{-4} \pm 0.2 \times 10^{-4}$ M^{-1}, respectively. The standard deviations of Kd_{1app} and Kd_{2app} were derived from Kd_{1app} and Kd_{2app} values, calculated by the Monte Carlo simulation using 100 sets of titration data in which the chemical shift value of each titration point independently contained a random error (the standard deviations of the experimental errors were set at 0.005 ppm). The results indicated that the difference between Kd_{1app} and Kd_{2app} was not significant, and the equilibrium system of the Cd(II)-binding process could be interpreted as that of two binding sites with the same *K*d value, as well. Because of the condensation of Cd(II) ions around an RNA oligomer and the resulting nonspecific Cd(II) ion-binding due to the electrostatic interaction between RNA oligomers and Cd(II) ions, the above dissociation constants are apparent values under the conditions that we measured, and the calculated values of Kd_{1app} and Kd_{2app} may have systematic errors.[9] For further realistic calculation, the charge condensation effect must be incorporated into the least-squares calculation. However, we could not perform such a complicated calculation due to the limitation of the program.

by ^{1}H NMR titration spectra, since the resulting theoretical curves were well fitted to the observed ^{15}N-chemical shifts (Figure 5). Therefore, chemical shift changes in N7/G1, N7/G2, N7/G5, and N7/G7 were cooperative, and transitions in theoretical curves for N7/G1, N7/G2, and N7/G5 should be the secondary effect caused by the Cd(II) ion-binding to the motif (Figure 5). Even when the motif was almost saturated by Cd(II) ions, Cd(II)-dependent chemical shift changes were observed in theoretical curves for all N7 nuclei, which means all the ^{15}N-chemical shifts converged on the asymptotes with linear slopes (Figure 5). Without this slope, theoretical curves did not fit to the observed chemical shift values very well. Therefore, apparent chemical shift changes for N7/G1 and N7/G2 should be mainly due to ionic strength dependent chemical shift changes and partly due to conformational changes, although there may be another possibility for the slopes.

Excluding these other sources of chemical shift changes, more than 12 ppm of the high-field shift of N7/G7 is directly attributable to the Cd(II) binding (Figure 5). Thus, the binding of Cd(II) to GA10 is N7/G7 specific. In the case of hydrogen bonding of N7 by Hoogsteen base-pairing in triplex DNA oligomers, N7 resonance of the guanosine residue was shifted toward high-field by only 8.5 ppm.[4a] Hence, the chemical shift perturbation of N7/G7 by the $CdCl_2$ titration is much larger than that caused by hydrogen bonding. This implies that N7/G7 strongly interacts with the Cd(II) ion and probably indicates inner-sphere coordination of the ion.

Discussion

From ^{15}N NMR spectra, we found that the chemical shift change upon addition of Cd(II) was N7/G7 specific. It was also observed that the resonance of N7/G7 was significantly broadened while the A9-G10.1 motifs were partially saturated by Cd(II). This broadening during the transition seemed to be due to the exchange between Cd(II)-bound and Cd(II)-unbound states, since the chemical shift difference between these states is quite large (19.6 ppm, 1.6 kHz). At this moment, we could not definitely derive a reason for the broadening, although we have tried to identify the origine in several ways. However, the resonance broadening was also N7/G7 specific and one of the interesting phenomena for the metal ion-binding site.

In the cases of the resonances of other nitrogen atoms, their chemical shift perturbations were much smaller than that of N7/G7, and thus these nitrogens are not ligands to the metal ions. Nevertheless, their chemical shift perturbations are quite informative. For example, the exocyclic amino group (N2) of G7 was shifted toward low-field upon addition of Cd(II) ions, which may suggest a strengthening of the hydrogen bond at this site.[4a,b,e] In some crystal structures of hammerhead ribozymes, the G10.1 residue (G7 in GA10) was rotated around its C1′ atom toward the major groove.[1b,c] In such a case, a short hydrogen bond between the amino group (N2) and keto-oxygen (O2) of C11.1 (C4 in GA10) or between the amino group (N2) and N3 of C11.1 was formed, and the hydrogen bond of the amino group would be strengthened. Alternatively, there still remains the possibility that this perturbation merely reflects a conformational change. It is also interesting that the resonance of the imino-nitrogen (N1) of G5 resonates at a higher field than the other imino-nitrogen throughout the titration experiments, and that the resonance of N2/G5 resonates at a lower field than the other amino-nitrogen (N2) throughout the experiments, which are characteristic features of a sheared type G−A pair.[4b] Therefore, sheared type G−A pairs were conserved, irrespective of whether metal ions bind to the motif or not. These data are consistent with the previous NOE titration data.[1i] Finally, the chemical shifts of N2-, N3-, and N9-nitrogens of the G7 residue were perturbed in quite different ways from those of other guanosine residues. This indicates that binding of the

(9) Misra, V. K.; Draper, D. E. *J. Mol. Biol.* **1999**, *294*, 1135−47.

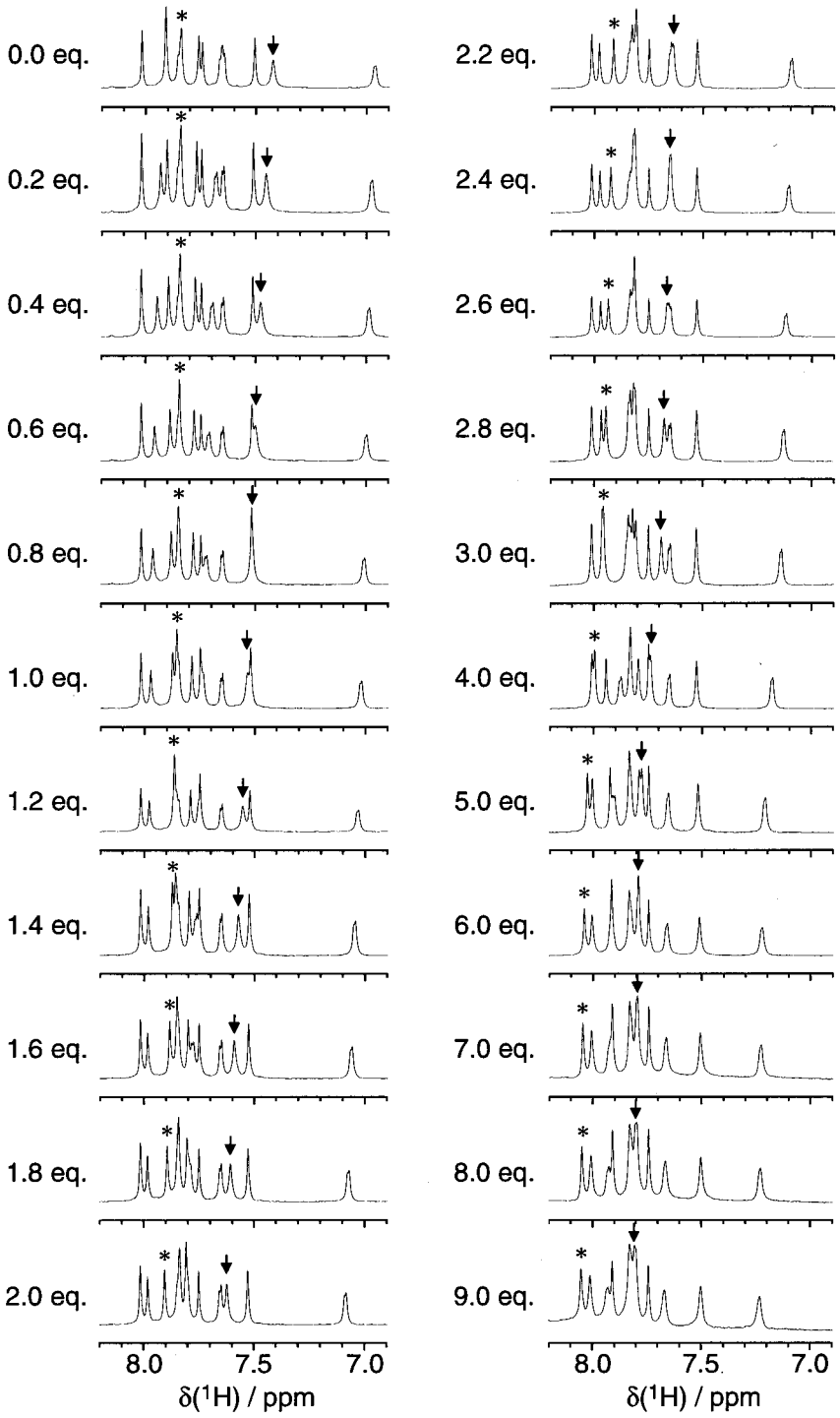

Figure 3. 1D ^{1}H NMR titration spectra of unlabeled GA10. The resonances of H8/G7 and H8/A6 are labeled by an arrow and an asterisk, respectively. The characteristic features of the H8/A6 resonance are described in the Results section. The titration experiments were performed at 313 K under the solution conditions of 1.5 mM GA10 (single strand), 40 mM $NaClO_4$, and various concentrations of $CdCl_2$ (0.2, 0.4, 0.6, 0.8, 1.0, 1.2, 1.4, 1.6, 1.8, 2.0, 2.2, 2.4, 2.6, 2.8, 3.0, 4.0, 5.0, 6.0, 7.0, 8.0, and 9.0 molar equiv to double stranded RNA oligomer). All the spectra were recorded on a Bruker DMX 800 spectrometer with spectral width of 10 000 Hz digitized into 16 384 complex points; 128 scans were averaged. These spectra were processed with an exponential window function to give a line-broadening of 3 Hz. Assignments of proton resonances were reconfirmed by 2D NOESY spectra at the ratios of $[CdCl_2]/[GA10(duplex)] = 0.8$ and 4.0. These assignments were also consistent with the results of $^1H-^{13}C$ HSQC spectra of labeled samples.

Cd(II) ion changes the electron density distribution of the guanine base of G7.

In the present work, the chemical shifts of the base proton and carbon of G7 (H8/G7 and C8/G7) showed significant low-field shifts as observed in our previous work,[1i] but the induced chemical shifts were much larger than those observed previously, namely, they are 2.3 (C8/G7) and 0.38 ppm (H8/G7) for Cd(II) ion-saturated conditions, and 1.1 (C8/G7) and 0.18 ppm (H8/G7) at the ratio of GA10(duplex):$CdCl_2$ = 1:2 at this time (unpublished data), whereas the corresponding values were 0.8 and 0.08 ppm at the ratio of GA10(duplex):$CdCl_2$ = 1:2 in the previous study. In the previous work,[1i] $MgCl_2$ was added prior to the addition of $CdCl_2$. This reduced the apparent perturbation due to the Cd(II) binding since the C8/G7 and H8/G7 resonances

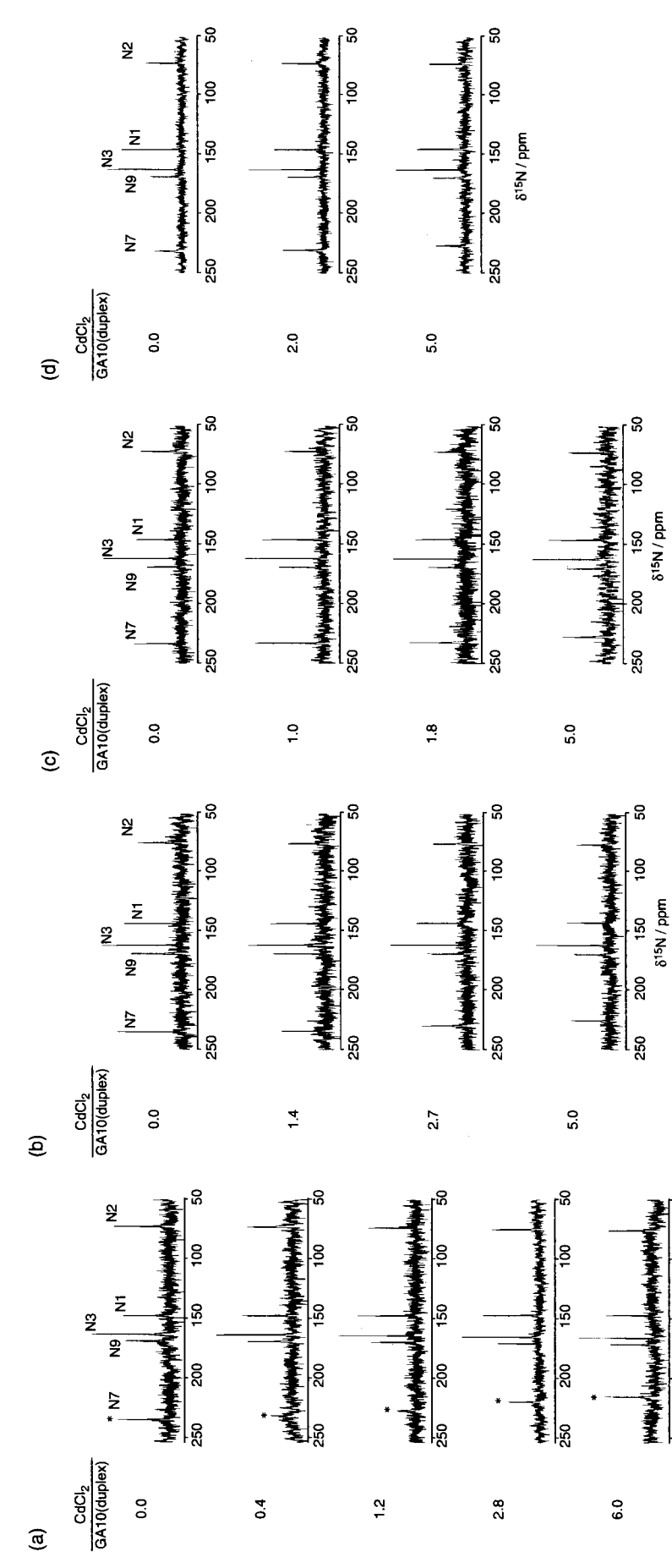

Figure 4. One-dimensional (1D) ^{15}N NMR spectra of (a) GA10G7L (0.9 mM as a single strand), (b) GA10G5L (0.74 mM as a single strand), (c) GA10G2L (0.68 mM as a single strand), and (d) GA10G1L (1.2 mM as a single strand) recorded at various concentrations of $CdCl_2$. In the crystal structures of hammerhead ribozyme, the metal ions were captured by N7 of the G10.1 residue, which corresponds to the G7 residue in GA10G7L.[1a−c] The ratios of $[CdCl_2]/[GA10(duplex)]$ are indicated on the left of each spectrum. All the resonances are labeled with the names of the nuclei in the spectrum at the top. The resonances of N7/G7 are labeled with an asterisk. Typical acquisition parameters were 313 K and a spectral width of 20 000 Hz digitized into 16 384 points (1.2 Hz/point and 0.015 ppm/point); 20 ,000 scans were averaged. These spectra were processed with an exponential window function to give a line-broadening of 10 Hz. The molar equivalency between the labeled RNA oligomer and Cd(II) ions was further calibrated by comparing respective 1D ^{1}H and ^{31}P NMR spectra of labeled samples at each solution condition with those of unlabeled RNA oligomer at various concentrations of $CdCl_2$. ^{15}N NMR titration experiments were performed until the $[CdCl_2]/[GA10(duplex)]$ ratio exceeded 5, since the preliminary ^{1}H NMR titration experiments were almost saturated at the ratio of 5 (Figures 2 and 3).

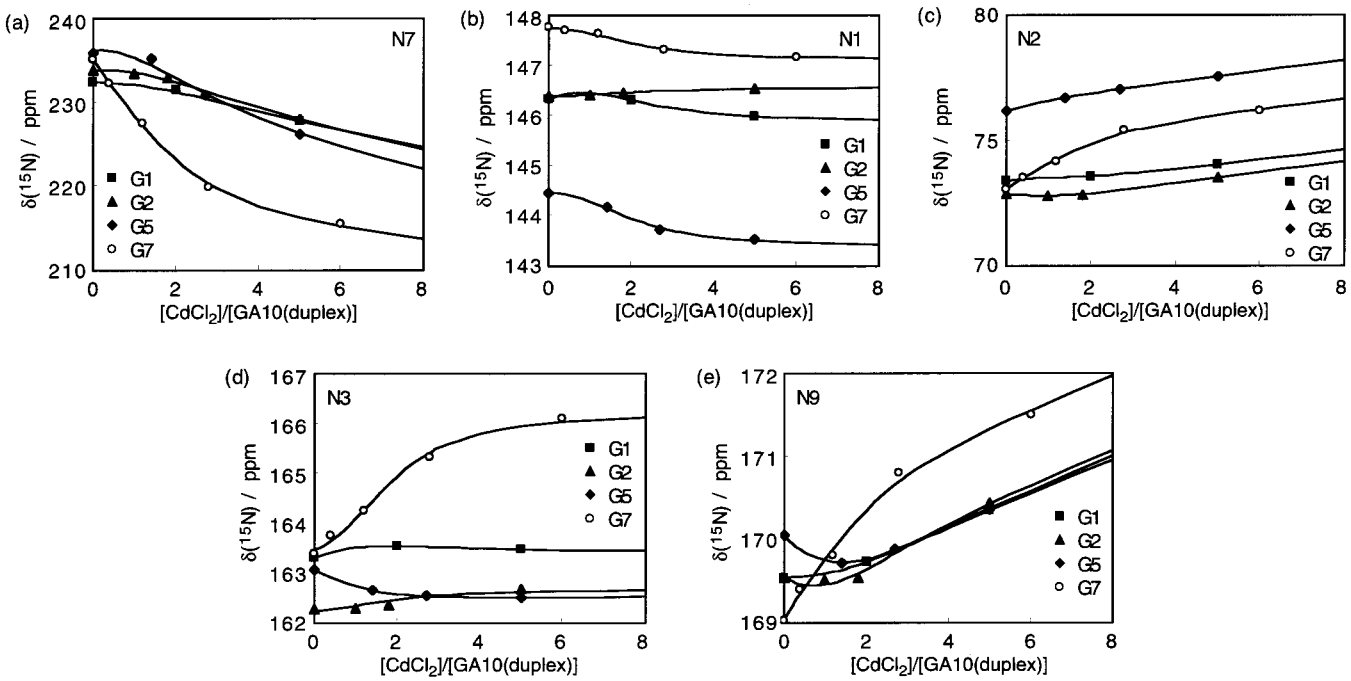

Figure 5. Chemical shifts of ^{15}N-nuclei are plotted against the molar ratio ([$CdCl_2$]/[GA10(duplex)]), according to the kind of nucleus for N7 (a), N1 (b), N2 (c), N3 (d), and N9 (e). Squares, triangles, diamonds, and open circles represent G1, G2, G5, and G7, respectively. The theoretical curves were generated, based on the result of the 1D ^{1}H NMR titration experiment. Chemical shift changes for all the nuclei were accountable for the same thermodynamic parameters, and found that spectral changes were cooperative. This indicates that chemical shift changes reflect metal ion-binding to the motif and resulting conformational changes for all sites.

were already shifted to low field by the $MgCl_2$. When compared with the perturbations due to Mg(II) binding, the perturbations due to Cd(II) ions were much larger and probably reflect the much stronger binding of the Cd(II) ion to the motif. This stronger interaction results in the quite large low-field shift of the C8/G7 and H8/G7 resonances. More importantly, the simultaneous large low-field shifts of the resonances of the base protons and base carbons indicate the binding of the metal ion to the N7-nuclei of the purine base. In the case of ^{31}P-nuclei, the resonance of the ligand phosphate group to the metal ion showed the largest shift (0.86 ppm toward high-field; unpublished data). In our previous paper,[1i] we could not unequivocally assign the ^{31}P-resonances in the presence of $CdCl_2$. In the present work, we found that the resonance of P/A6 of GA10, which corresponds to P/A9 in the hammerhead ribozyme, shifted toward high-field upon addition of $CdCl_2$, for the first time. This shift is also much larger than that due to Mg(II) binding.

Now, we discuss the scalar coupling between ^{113}Cd(II) ion and ^{15}N-nucleus of N7/G7. Scalar coupling through hydrogen bonds has been observed between hydrogen-bonded nitrogen atoms ($N-H\cdots N$).[4c,d] In addition, an inner-sphere coordination is a much stronger interaction than hydrogen bonding. Therefore, scalar coupling between ^{113}Cd(II) ion and ^{15}N7/G7 should be observed if the Cd(II) ion is directly coordinated to N7/G7. Actually, large scalar couplings were observed between ^{113}Cd(II) and ^{15}N (78−216 Hz) in cadmium *meso*-tetraphenylporphyrin and the complex between β-lactamase and Cd(II) ion.[5] Thus, we tried to observe the scalar coupling between ^{15}N7/G7 and ^{113}Cd(II) ($I = {}^1/_2$). However, no scalar coupling was observed. Nevertheless, the existence of scalar coupling and the possibility of inner-sphere coordination of the Cd(II) ion cannot be excluded since the ^{15}N resonance was quite broad. The line width at half-height ($\nu_{1/2}$) was 22 Hz for N7/G7 at Cd(II) saturation and ~100 Hz when unsaturated due to scalar coupling with ^{13}C-nuclei and the chemical exchange, and thus a scalar coupling smaller than the line width would not be detectable. It is noted that scalar couplings in complexes between nucleosides and the ^{199}Hg(II) ion have previously been found difficult to observe,[6a,b] and as a consequence, there is some controversy over whether metal ion-binding to nucleic acids involves inner-sphere coordination.[6a,b] The failure to observe scalar coupling between ^{113}Cd(II) and ^{15}N may be due to the fast exchange of the ion between the free and bound forms.[6a,b] If present, the scalar coupling constant would be smaller than 20 Hz for our sample at the metal ion-saturated condition, which would be much smaller than previously observed constants.[5]

However, ^{15}N-chemical shift perturbation by 19.6 ppm is quite large and one of the largest shifts of all metal ion−nucleic acids system ever observed. In conclusion, we were able to unambiguously identify N7/G7 as the Cd(II) binding site in a model-independent manner.

Experimental Section

Uniformly ^{15}N- and ^{13}C-labeled guanosine phosphoramidite was synthesized from uniformly ^{15}N- and ^{13}C-labeled guanosine as described elsewhere.[4e,7] RNA oligomers labeled with a specific single nucleotide were chemically synthesized, and purified as previously described (Figure 1d).[1i,4e] All the RNA oligomers were quantitated by UV absorbance at 260 nm after nuclease P1 digestion. The error in the quantitation is less than 3%, which is important for the titration experiments in which the molar ratio is critical.

The solutions for NMR measurements contained 0.63−1.5 mM GA10, 40 mM $NaClO_4$, and various concentrations of $^{113}CdCl_2$. To avoid precipitation of metal−buffer complexes and the resulting pH changes, no buffer was added to the solution used in the NMR measurements.[1i] Instead, the pH of each solution was adjusted to 6 by direct titration as described previously.[1i] All titration experiments were performed at 313 K. In this paper, we chose $CdCl_2$ as the divalent cation source, since $MgCl_2$ induces intermolecular aggregation and

significant signal broadening at Mg(II)-saturating conditions,[1i] and also because all of the proton resonances were sharp and traceable until Cd(II) ion excess conditions. Further, in the favorable cases for labeled samples, the scalar coupling between ^{15}N-nuclei of N7/G7 and ^{113}Cd(II) ions could be observed. For the monovalent cation source, $NaClO_4$ was employed instead of NaCl since chloride ions bind to Cd(II) ions and cause further signal-broadening of ^{113}Cd NMR spectra due to the quadrupolar nuclei of chloride ions ($^{35}Cl^-$ and $^{37}Cl^-$ ions). The chemical shift value of Cd(II) was included in the ranges of those of hexacoordinated Cd(II) complexes. However, more precise information were not derived, since the chemical shift of Cd(II) is affected by so many factors such as the binding of ligands (nucleobases, phosphates, and Cl^- ions) and the concentration of Cd(II) itself. The conditions for NMR measurements are presented in the legends to Figures 3 and 4.

For the generation of the theoretical curves for ^{15}N-chemical shift changes, the solution equilibrium for the Cd(II)-GA10 system was analyzed by 1D ^{1}H NMR titration spectra. Here we assumed double transitions between three states (free GA10, GA10 with a single Cd(II) ion, and GA10 with two Cd(II) ions) (eqs 1 and 2), since several signals were not well described using only a single transition between two states (free GA10 and GA10 with two Cd(II) ions)

$$\text{GA10} + \text{Cd(II)} \overset{K\text{d}_{1\text{app}}}{\rightleftharpoons} \text{GA10·Cd(II)} \quad (1)$$

$$\text{GA10·Cd(II)} \overset{K\text{d}_{2\text{app}}}{\rightleftharpoons} \text{GA10·2Cd(II)} \quad (2)$$

where GA10, Cd(II), GA10·Cd(II), GA10·2Cd(II), $K\text{d}_{1\text{app}}$, and $K\text{d}_{2\text{app}}$ mean GA10(duplex), Cd^{2+} ion, the 1:1 complex between GA10(duplex) and Cd(II), the complex between GA10(duplex) and two Cd(II) ions, an apparent dissociation constant for the first Cd(II) binding, and an apparent dissociation constant for the second Cd(II) binding. Nonlinear least-squares regression was performed with Excel 98 on a Macintosh, based on the following equations:[4e,8]

$$K\text{d}_{1\text{app}} = \frac{[\text{GA10}][\text{Cd(II)}]}{[\text{GA10·Cd(II)}]} \quad (3)$$

$$K\text{d}_{2\text{app}} = \frac{[\text{GA10·Cd(II)}][\text{Cd(II)}]}{[\text{GA10·2Cd(II)}]} \quad (4)$$

$$[\text{GA10}]_t = [\text{GA10}] + [\text{GA10·Cd(II)}] + [\text{GA10·2Cd(II)}] \quad (5)$$

$$[\text{Cd(II)}]_t = [\text{Cd(II)}] + [\text{GA10·Cd(II)}] + 2[\text{GA10·2Cd(II)}] \quad (6)$$

$$\delta_{\text{calc}} = \delta_{\text{f}}\frac{[\text{GA10}]}{[\text{GA10}]_{\text{t}}} + \delta_{\text{m}}\frac{[\text{GA10·Cd(II)}]}{[\text{GA10}]_t} + \delta_{\text{d}}\frac{[\text{GA10·2Cd(II)}]}{[\text{GA10}]_{\text{t}}} \quad (7)$$

$$f = (\delta_{\text{obs}} - \delta_{\text{calc}}) \quad (8)$$

where $[GA10]_t$, $[Cd(II)]_t$, [GA10], [GA10·Cd(II)], [GA10·2Cd(II)], [Cd(II)], δ_{calc}, δ_{f}, δ_{m}, δ_{d}, δ_{obs}, and f are the total concentrations of GA10(duplex), and Cd(II), the equilibrium concentrations of GA10(duplex), GA10·Cd(II), GA10·2Cd(II), and Cd(II), the calculated chemical shifts of the specific proton of GA10(duplex), free GA10(duplex), monometalated GA10(duplex), and dimetalated GA10(duplex), the observed chemical shift of the corresponding proton, and the target function to be minimized for the least-squares calculation, respectively. Experimental data and theoretical curves for 1D ^{1}H NMR titration spectra are presented in Figure 2. Based on the results from ^{1}H NMR titration spectra, the least-squares fittings for ^{15}N-chemical shifts were performed, and their resulting theoretical curves are presented in Figure 5.

Acknowledgment. The authors would like to thank Prof. Uesugi and Dr. Katahira, Yokohama National University, for helpful comments, and Drs. Nakanishi, Nemoto, and Ishizuka, AIST, for technical advice. Y.T. was supported by a Domestic Research Fellowship (Japan Science and Technology Corporation). This work was supported in part by CREST of JST.

JA011520C